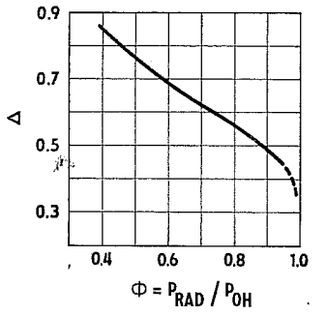

Fig. 5. Computed relation between the width of radial profile of the electron temperature Δ and the parameter $\phi = P_{RAD}/P_{OH}$ demonstrating the peaking of the electron temperature if radiative losses increase. Profile of T_e is supposed in the form $T_e = T_e(0) \exp(-x^2/\Delta^2)$, $x = r/a$.

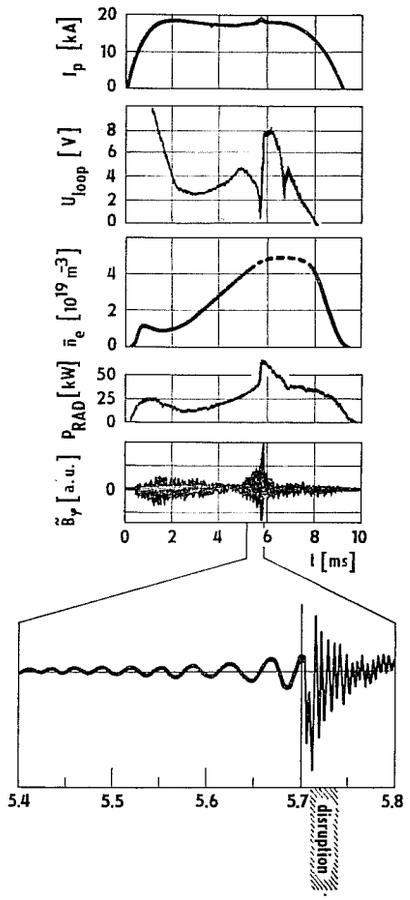

Fig. 6. Time evolution of a high density discharge with a minor disruption at $t = 5{\cdot}7$ ms. I_p — plasma current, U_{loop} — loop voltage, P_{RAD} — radiative power losses, $\bar{n}_e$ — plasma density, $\tilde{B}_\varphi$ — signal from a magnetic probe registering fluctuations of the poloidal magnetic field.

losses and plasma MHD activity during the discharge with a disruptive instability at time $t = 5{\cdot}7$ ms. As the toroidal current changes only slightly during the instability, we can characterize this instability like the "minor" one according to the Kadomtsev classification [9]. It may be seen that while the radiative losses follow the plasma density increase until the disruption (in the same way as during the stable discharge), they increase suddenly at the moment of instability. In contrast to the MHD activity, no precursor on the curve P_{RAD} before the negative spike of the loop voltage is observed. Simultaneously a small increase of the toroidal current and a negative loop voltage spike indicate a fast decrease of the plasma column inductance (fast inward motion of the current channel and maybe its expansion as well). Moreover, after the disruption the hard X-ray radiation (HXR) observed during the discharge (not shown in fig. 6) disappears. It indicates an escape of high energy electrons from the plasma.

To show the operating region of the CASTOR tokamak, we present the stability diagram [8] in fig. 7. The hatched area corresponds to the unstable discharges.

The quantity $\bar{n}_{cr}$ is a critical density above which the discharge becomes unstable. The parameter $\bar{n}_{cr} \cdot R/B_T$ is related to the relative level of radiation $\phi = P_{RAD}/P_{OH}$, as it has been shown in [7].

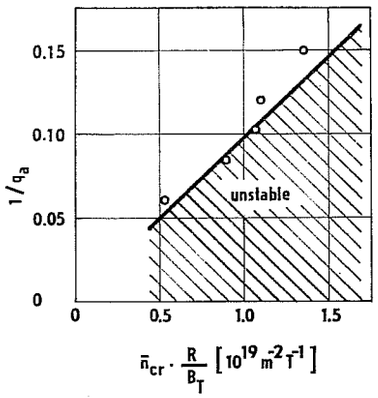

Fig. 7.

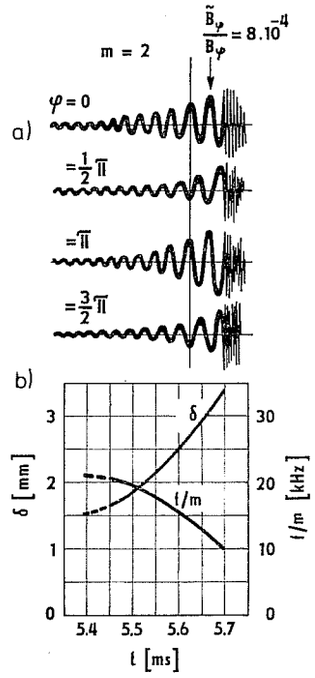

Fig. 8.

Fig. 7. Hugill plot of density limit disruption for the CASTOR tokamak ($R = 0{\cdot}4$ m, $B_T = 1{\cdot}3$ T).

Fig. 8.a) Comparison of signals from four magnetic probes uniformly distributed around the liner in a poloidal cross-section. Correlation of the signals indicates a growth of the $m = 2$ mode before disruption. φ — poloidal angle. b) Time evolution of the width δ of the magnetic island $m = 2$ and frequency of the oscillations f/m for the corresponding mode number.

Fig. 8a shows oscillograms of signals from the four magnetic probes, uniformly distributed around the liner in a poloidal cross-section and registering the disturbance $\tilde{B}_\varphi$ of the poloidal magnetic field B_φ. Quite regular oscillations corresponding to the $m = 2$ mode before disruption can be seen in fig. 8a.

In fig. 8b the time dependence of the frequency of the oscillations for the corresponding mode number f/m and the island width δ estimated as $\delta = b\sqrt{(\tilde{B}_\varphi/B_\varphi)}$ [10] from oscillograms in fig. 8a are given. The radius of magnetic coil position is denoted by b. The island width δ evaluated in such a way increases rapidly approaching the disruption and its maximum value reaches (3–4) mm. Simultaneously frequency of the oscillations decreases. The increase of δ may be connected with a sharpening of the current density profile. In fig. 9 a calculated dependence of the